Acoustic properties and density of polyurea at pressure up to 13.5 GPa through Brillouin scattering spectroscopy

T. C. Ransom,[1,a)] Muhtar Ahart,[2] Russell J. Hemley,[2] and C. M. Roland[1,b)]
[1]*Naval Research Laboratory, Chemistry Division, Code 6105, Washington DC 20375-53452, USA*
[2]*Institute of Materials Science and Department of Civil and Environmental Engineering, The George Washington University, Washington DC 20052, USA*

(Received 29 March 2018; accepted 1 May 2018; published online 18 May 2018)

Brillouin scattering was performed on an elastomeric polyurea, an important technological polymer. Being widely used for impact modification, of particular interest is its response to extreme pressure conditions. We applied pressures up to 13.5 GPa using a diamond anvil cell and measured the longitudinal and transverse sound velocities via Brillouin light scattering. From these data, the equation of state, the elastic moduli, and Poisson's ratio were obtained. By comparison with previous dilatometry measurements up to 1 GPa, we show how viscoelastic effects can be accounted for in order to obtain an accurate equation of state. Because of the extreme strain-rate hardening of vitrifying polyurea, the property changes associated with its solidification are more subtle in the high frequency Brillouin data than observed in conventional mechanical testing and dilatometry. *Published by AIP Publishing*. https://doi.org/10.1063/1.5031427

INTRODUCTION

The past decade has seen a dramatic increase in the use of pressure as an experimental variable, particularly in the study of amorphous liquids and polymers.[1,2] The interpretation of high pressure data usually requires knowledge of the density, ρ, for measurements performed as a function of temperature, T, and pressure, P, that is, the equation of state (EoS), $\rho(T,P)$, is required. A prominent recent example of this is thermodynamic scaling of dynamic quantities and transport properties, in which measurements at various T and P are expressed as a function of $T\rho^{\gamma_s}$, in which γ_s is a material constant related to the intermolecular repulsive potential.[3–5] Polyurea is a technologically important polymer, which has seen increasing use as a coating for infrastructure protection and military armor.[6,7] Because of its application as an impact coating, much work has been done characterizing the properties of polyurea under extreme conditions, such as high strain rates and high pressures.[6–19] It is therefore of interest to determine its density and mechanical properties for large compressive forces.

Measuring the EoS of amorphous systems is substantially more difficult than for crystalline materials. The density of the latter can be obtained from x-ray and neutron diffraction, but these methods are not applicable to materials lacking long range order. In high pressure work, Bridgman measured the EoS for many amorphous materials using dilatometry, in which a piston-cylinder apparatus or a sample within a confining fluid was employed.[20] Zoller *et al.* reported the *P-V-T* results for many polymers by the latter method, but most of the data were limited to 0.2 GPa.[21]

Diamond anvil cell (DAC) methods together with an expanding range of measurement techniques are now capable of determining the properties of materials up to several hundred GPa.[22] Standard dilatometry techniques are challenging in a DAC, but Brillouin light scattering can be used to obtain density changes from changes in the acoustic sound velocities.[23–27] An acknowledged problem with this technique, however, is that Brillouin scattering probes materials at very high (GHz) frequencies, and polymers, which are viscoelastic, exhibit sound velocities (and mechanical properties) that are invariably strongly dependent on frequency.[28,29] Neglect of this effect leads to an underestimation of density changes in the typical isothermal compression experiment; nevertheless, no corrections for viscoelasticity have been applied in previous high pressure Brillouin scattering studies of polymers.

In a recent study of polyurea, we measured the glass transition temperature, T_g, up to 6 GPa using a DAC technique based on the disappearance of pressure gradients in a glassy sample upon heating through T_g.[30] At 22 °C, the polymer vitrifies at 1.1 GPa. The EoS for the polyurea up to 1 GPa was also obtained using dilatometry.[30] In this work, we report the density and moduli of the same polyurea at pressures up to 13.5 GPa from Brillouin measurements using a DAC. While the theory of Brillouin scattering is described in detail elsewhere,[31] we briefly discuss pertinent aspects herein. In any material, thermally generated acoustic phonons, having a range of momenta, are continuously created and destroyed. Incident laser light can absorb or create such a phonon, resulting in a shift in frequency $\pm\upsilon$ and momentum of the scattered photon. By collecting light along a well-defined scattering angle, conservation of momentum restricts the phonons probed to a specific momentum q. Longitudinal acoustic (LA) phonons at this q have a peak frequency υ_L and phase velocity v_L determined by the elastic properties of the medium. Transverse acoustic (TA) phonons with frequency υ_T and velocity v_T can also propagate if the viscosity is high enough to transiently support a shear wave. Scattering from these phonons gives rise to symmetric peaks in the resulting frequency spectrum. Conservation of energy

[a)]Electronic mail: timothy.ransom.ctr@nrl.navy.mil
[b)]Electronic mail: mike.roland@nrl.navy.mil

and momentum yields an equation specific to equal-angle forward scattering[32]

$$\upsilon_i = \frac{2v_i}{\lambda_0}\sin\left(\frac{\theta}{2}\right) \tag{1}$$

in which λ_0 is the wave length and θ the scattering angle. This equation is used to calculate sound velocities v_i from peak positions υ_i.

We show herein that the effect of viscoelasticity on the bulk modulus is significant, causing the Brillouin values to be substantially larger than obtained from low frequency dilatometry experiments. We provide a correction for this effect to obtain accurate densities in agreement with the lower pressure dilatometry data.[30] As expected, the longitudinal modulus increases strongly with pressure, with a change in pressure-sensitivity upon vitrification.

EXPERIMENTAL METHODS

Polyurea was prepared by a reaction of Versalink P1000 polyamine (Air Products) with Isonate 143 L isocyanate (Dow Chemical) in a 4:1 mass ratio. Films 100–200 μm thick were prepared by pressing the reactants between Teflon sheets, followed by curing for 8 h at 75 °C. The sample was then allowed to equilibrate under ambient conditions, with a consequent small water uptake (<1% by weight). Small discs were cut from the molded sheet and loaded into a DAC using a stainless steel gasket. One or two ruby chips were also positioned in the sample cell (dimensions approximately 300 μm in diameter and 60 μm thick) for *in-situ* pressure determination.[33] Ruby fluorescence spectra were collected using a Princeton Instruments Acton SP2300 spectrometer with an 1800BLZ grating, giving a pressure uncertainty of ±0.1 GPa. The experiments were repeated thrice, each with a separate sample loading.

Brillouin spectra were collected using a single-mode, Ar-ion laser ($\lambda_0 = 514.5$ nm) as an excitation source. The laser power was kept below 100 mW; nevertheless, some minor photodegradation of the polyurea was observed. Light from the DAC was collected in a symmetric, equal angle forward scattering geometry (external scattering angle = 61.61°). The scattered light was focused onto a 100 μm pinhole of a 3 + 3 tandem Fabry-Perot interferometer. A schematic of the experimental setup is shown in Fig. 1. A typical spectrum was collected for 20–60 min at each pressure, with longer collection times at higher pressures due to the weaker signal. Measurements herein

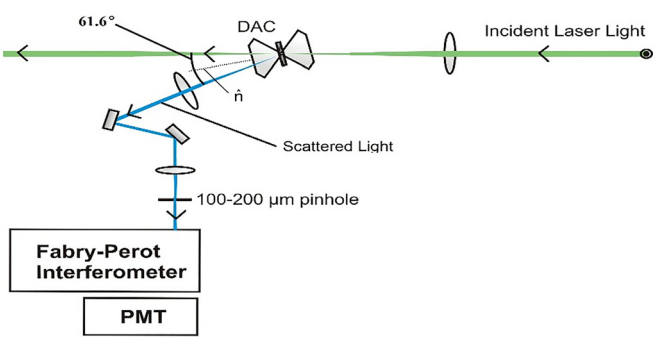

FIG. 1. Experimental setup for Brillouin light scattering in a DAC.

were at room temperature (22 °C), at pressures from 0.1 MPa to 13.5 GPa. Typically, pressures were systematically increased although a cyclic compression/decompression measurement gave no indication of hysteresis.

RESULTS AND ANALYSIS

Typical Brillouin spectra are shown in Fig. 2, in which prominent LA mode peaks are evident; these shift to higher frequencies with pressure. Also present are the much weaker TA mode peaks. Being too low in frequency to be observed in the ambient pressure spectrum, they emerge from the central line at ~0.4 GPa. This appearance of the TA modes at high pressure is discussed in Ref. 23. The shift of the TA modes with pressure is much weaker than for the LA modes. The amplitudes of both peaks decrease at higher pressures. When the polyurea is deep in the glassy state (>5 GPa), the TA modes became too weak to resolve; however, the LA modes can be observed up to the highest pressures herein (>13 GPa).

To extract the peak frequencies υ_L and υ_T, spectra were fit with each mode modeled by a damped harmonic oscillator

$$I(\upsilon) = \frac{I_0}{(2\Gamma\upsilon)^2 + \left(\upsilon^2 - \upsilon_i^2\right)^2}, \tag{2}$$

where I_0 is the intensity and Γ the half width. Half widths decreased with pressure up to vitrification due to the increasing phonon lifetimes on compression. In the glassy state, there is an apparent broadening of the Brillouin doublets due to non-hydrostatic conditions (non-uniform local pressures). From the peak shift frequencies, the LA (v_L) and TA (v_T) sound velocities were calculated via Eq. (1) (Fig. 3). While both v_L and v_T increase monotonically with pressure, the effect is markedly stronger at low pressures (below 1 GPa). The pressure at which the response becomes glassy, $P_g = 1.1$ GPa at 22 °C for low frequencies,[30] is indicated in the figure.

Even though the TA modes are not visible in all spectra, the values of v_T for all pressures are required to calculate the

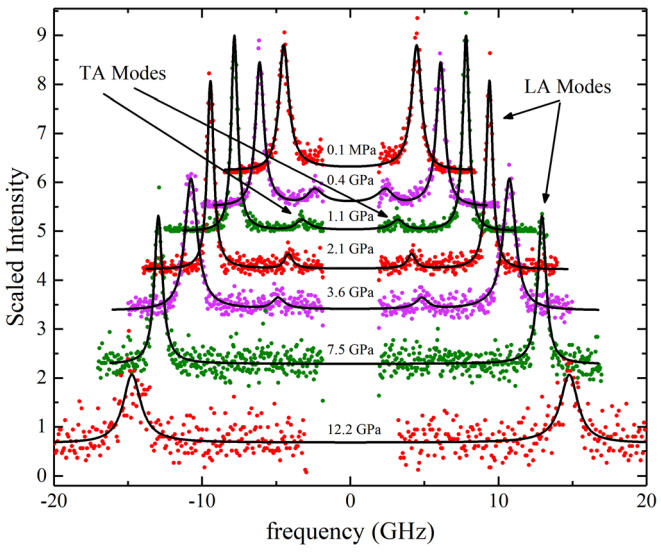

FIG. 2. Selected Brillouin spectra from polyurea showing the pressure evolution of longitudinal (LA) and transverse (TA) acoustic mode peaks. Solid lines are fits to Eq. (2).

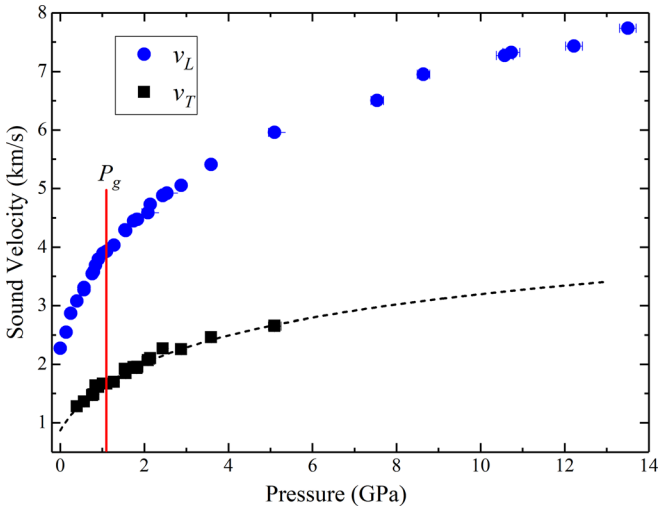

FIG. 3. Longitudinal and shear sound velocities for polyurea calculated from Eq. (1). Dashed line is the fit of Eq. (3). Vertical line denotes the glass transition pressure, $P_g = 1.1$ GPa at room temperature.[30] The error bars are no larger than the symbol size.

density ρ and elastic parameters. Therefore, the available v_T measurements can be fit with a phenomenological model

$$v_T(P) = v_{T0} + C_T \ln\left(1 + \frac{P}{b_T}\right), \tag{3}$$

where b_T and C_T are constants and $v_{T0}(T)$ is the sound velocity at zero pressure. To verify Eq. (3), we applied it to the data in Ref. 23 and found it to describe accurately the isothermal pressure dependence of v_L and v_T for three polymers over similar pressure ranges. The fit to v_T for polyurea shown in Fig. 3 yields $v_{T0} = 0.866 \pm 0.15$ km/s, $C_T = 0.855 \pm 0.076$ km/s, and $b_T = 0.7 \pm 0.2$ GPa. We then extrapolated to estimate v_T in the low (<0.4 GPa) and high (>5 GPa) pressure regimes.

In order to calculate ρ at high pressures using Brillouin sound velocity data, most studies use the equation

$$\rho - \rho_0 = \int_{P_0}^{P} \frac{\gamma}{v_B^2} dP', \tag{4}$$

where ρ_0 is the ambient density, γ the adiabatic index, and v_B the bulk sound velocity introduced for mathematical convenience[23,27,34]

$$v_B^2 = v_L^2 - \frac{4}{3} v_T^2. \tag{5}$$

However, Eq. (4) neglects the fact that Brillouin scattering measures sound velocities at very high (GHz) frequencies, which due to viscoelastic effects yields values higher than would be measured using a low frequency probe.[35] In polymers, the principal viscoelastic time constant is the local segmental relaxation time τ, defining the onset of glassy behavior.[1,2,29] When the time scale of a dynamic measurement is much longer than τ, the material response is liquid-like ("relaxed"), whereas solid-like behavior is observed for measurements occurring faster than the material response. In the case of the polyurea at room temperature, previous dielectric measurements reported $\tau \sim 1$ μs at 0.1 MPa.[36,37] Acoustic phonons measured by Brillouin scattering are in the GHz frequency range and thus probe the polymer on times scales of a few ns, i.e., much shorter than τ at ambient conditions. Since compression further increases τ, our Brillouin measurements are all in the unrelaxed, solid-like regime. In a study of liquid methanol for which $\tau \sim 1$ ns at ambient pressure, correction for viscoelastic effects was shown to change the response from that of a relaxed to an unrelaxed state with increasing pressure approaching vitrification.[38] Equation (4) is derived based upon the assumption of a relaxed response and cannot yield accurate densities if applied directly to our sound velocities herein. While Ref. 23 alluded to this problem, no attempt was made to estimate the error.

We derive a correction to Eq. (4) for the viscoelastic contribution, relying on the density measurements from dilatometry on this same polyurea to ~1 GPa.[30] These data were described by the Tait EoS[21]

$$\rho(P) = \rho_0(T)\left[1 - C \ln\left(1 + \frac{P}{B(T)}\right)\right], \tag{6}$$

where $\rho_0(T)$ was modeled with a 2nd degree polynomial, $B(T) = b_0 \exp(-b_1 T)$, and C is a constant. From this, we calculated the pressure dependence of the isothermal bulk modulus

$$K_T = \rho \left.\frac{dP}{d\rho}\right|_T, \tag{7}$$

and using the Maxwell relation, the low frequency adiabatic bulk modulus K_{S0}

$$\frac{1}{K_{S0}} = \frac{1}{K_T} - \frac{\alpha^2 T}{\rho c_P}, \tag{8}$$

where α is the thermal expansivity and c_P the isobaric specific heat capacity. We calculated α from the EoS and measured $c_P = 1.97$ J/g · K using differential scanning calorimetry (c_P was approximated as constant).

In contrast to the relaxed modulus K_{S0} obtained from dilatometry, Brillouin scattering determines (at least when τ is large) the high frequency adiabatic bulk modulus, $K_{S\infty} = \rho v_B^2$, which is the modulus in the unrelaxed limit. $K_{S\infty}$ can be modeled by

$$K_{S\infty} = K_{S0} + \Delta K_S, \tag{9}$$

where ΔK_S is the relaxing part of the modulus describing the increase at very high frequencies.[28] [The assumption of Eq. (9) that stresses are additive is open to question.[39]] Fig. 4 shows the values of $K_{S\infty}$ and K_{S0} from ambient pressure up to 1.1 GPa. It is apparent that $K_{S\infty}$ is significantly larger than K_{S0}; however, the curves are essentially parallel over the entire pressure range, indicating that the pressure-dependence is consistent for the two methods. Thus, the relaxing part is constant to within the uncertainty, $\Delta K_S = 1.56 \pm 0.23$ GPa. This value is used in subsequent calculations for $P < P_g$.

The viscoelastic effect is also evident by comparing the longitudinal modulus M and shear modulus G measured at different frequencies. In the inset of Fig. 4 are M and G at ambient conditions from ultrasonic spectroscopy at 1 MHz,[40] dynamic

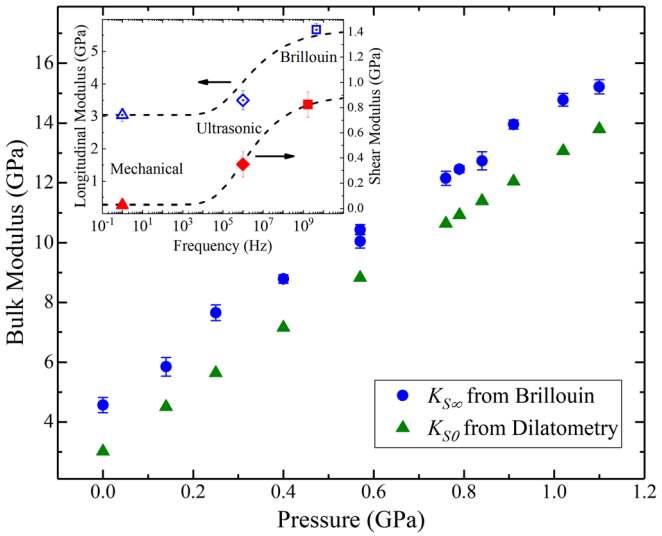

FIG. 4. Measurements of $K_{S\infty}$ from Brillouin data and K_{S0} calculated from the dilatometry measurements of Ref. 30 using Eq. (8). The two data points at P = 0.6 GPa are measurements from two separate DAC loadings, and thus a measure of the reproducibility. Inset shows the longitudinal modulus (open symbols; left ordinate) and shear modulus (solid symbols; right ordinate) measured at 0.1 MPa using dynamic mechanical,[19] ultrasonic,[40] and Brillouin scattering. Dashed lines represent the KWW function with $\beta_{KWW} = 0.3$.

mechanical spectroscopy at 1 Hz,[19] and the current Brillouin data at several GHz (calculated as $M = \rho v_L^2$ and $G = \rho v_T^2$). The moduli increase significantly with increasing measurement frequency. The dashed lines show data for a Kohlrausch-Williams-Watts (KWW) relaxation function[29] with a representative value of the stretch exponent, $\beta_{KWW} = 0.3$.

The adiabatic index can be obtained from the low pressure dilatometry data $\gamma = K_{S0}/K_T$. While γ is typically ~1.2 at ambient pressure, it decreases towards unity at high pressure.[23] Previous Brillouin studies often assumed $\gamma = 1$,[23,41] but from our values of K_T and K_{S0}, we calculate an ambient value $\gamma_0 = 1.12$, decreasing with pressure to asymptotically approach $\gamma_P = 1.08$. For pressures beyond the range of the EoS, we held γ constant at γ_P. The modeling of this parameter gives a more accurate calculation of density via Eq. (4) than the usual approximation $\gamma = 1$.

In order to incorporate ΔK_S in the calculation of ρ, we express K_T in terms of ΔK_S

$$K_T = \frac{K_{S0}}{\gamma} = \frac{1}{\gamma}(K_{S\infty} - \Delta K_S). \tag{10}$$

Inserting into Eq. (7) along with $K_{S\infty} = \rho v_B^2$ yields

$$d\rho = \frac{\rho\gamma}{\rho v_B^2 - \Delta K_S} dP, \tag{11}$$

which upon integration gives

$$\rho - \rho_0 = \int_{P_0}^{P} \frac{\gamma}{v_B^2}\left(1 - \frac{\Delta K_S}{\rho v_B^2}\right)^{-1} dP'. \tag{12}$$

This is Eq. (4) corrected for viscoelasticity. Since the integrand contains ρ, formally the integration is not allowed. However, we proceed by first obtaining an approximate $\rho(P)$ from Eq. (4) and then inserting those values into the integrand of Eq. (12). By iteration, we arrive at the most accurate values of $\rho(P)$.

The value determined for ΔK_S in Eq. (12) is strictly applicable only to the polyurea above T_g. In the glassy state, τ is so large that the density increases very slowly as the polymer equilibrates, a process known as physical ageing.[42] This means that our experimental time scale (i.e., time for a pressure increment and spectral measurement, tens of minutes) is much shorter than τ for the glassy polyurea; thus, a pressure change induces a density response according to K_∞ rather than K_0. Accordingly, we set $\Delta K_S = 0$ for pressures higher than $P_g = 1.1$ GPa.

The integration of Eq. (12) yields $\rho(P)$ up to 13.5 GPa, as displayed in Fig. 5. Note that the values obtained with Eq. (12) are much more consistent with the low pressure dilatometry data than using Eq. (4), which does not correct for viscoelasticity. In Ref. 23, Brillouin measurements were used to calculate $\rho(P)$ using Eq. (4) for three other polymers up to about 14 GPa. When compared with lower pressure dilatometry data, these $\rho(P)$ values were found to be significantly too low. However, we find that these differences vanish when the data are analyzed via Eq. (12) with estimates of ΔK_S. The parameter ΔK_S is applicable to any material exhibiting a viscoelastic response although of course its value would be material dependent. The aforementioned finding that ΔK_S is constant is important because it suggests that it is sufficient to have a single determination of K_{S0} at ambient pressure in order to apply Eq. (12). This would be useful for a Brillouin study of a material for which dilatometric characterization is lacking.

Many different EoS models have been used to describe the pressure dependence of ρ; for example, Ref. 23 compared five EoS for their ability to fit data. Herein, we report results for the Tait EoS, Eq. (6), used previously for dilatometry data.[30] For an isothermal pressurization at $T = 22\,^{\circ}$C,

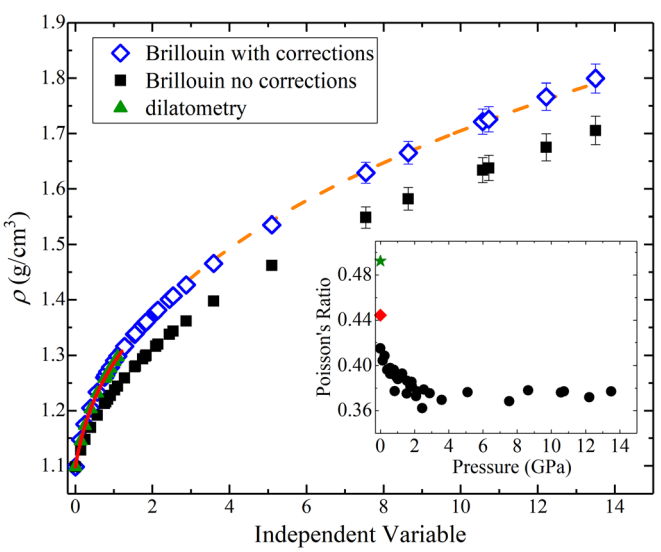

FIG. 5. Pressure dependence of ρ for polyurea calculated with viscoelastic corrections [Eq. (12)] and without corrections [Eq. (4)]. Dilatometry values are from Ref. 30; solid and dashed lines are fits of Eq. (6) to data below and above P_g, respectively. Inset shows Poisson's ratio determined from: Brillouin (circles), dynamic mechanical at 1 Hz[19] (star), and ultrasonic at 1 MHz[40] (diamond).

TABLE I. Parameters from fits of **Eq. (6)**.

	C	B (GPa)
$P < 1.1$ GPa	0.0889±0.001	0.239±0.007
$P > 1.1$ GPa	0.1058±0.001	0.358±0.007

only the parameters C and B were adjusted in fitting the data, with the ambient density fixed at ρ=1.098 g/ml. We fit separately the regimes above and below P_g, using for the latter the parameters from Ref. 30; results are given in Table I. As seen in Fig. 5, the Tait equation accurately describes the densities for both rubbery and glassy polyurea.

Using the EoS for the entire pressure range, we calculated the pressure dependence of the high frequency longitudinal and shear moduli via the relations $M_\infty = \rho v_L^2$ and $G_\infty = \rho v_T^2$; these are shown in Fig. 6. There is a marked decrease in the sensitivity to pressure above P_g, the weaker dependence due to the reduced compressibility of the glass.

From the ratio of transverse to longitudinal strain, we calculate Poisson's ratio

$$\tilde{\nu} = \frac{v_L^2 - 2v_T^2}{2v_L^2 - 2v_T^2}, \tag{13}$$

which is plotted versus pressure in the inset of Fig. 5. From a value of 0.41 at ambient, $\tilde{\nu}$ decreases to 0.37 over the first few GPa, remaining constant for higher pressures. The neglect of viscoelasticity also reduces the magnitude of the apparent $\tilde{\nu}$. From ultrasonic measurements at 1 MHz,[40] $\tilde{\nu} = 0.44$.

CONCLUSIONS

Using Brillouin scattering, the longitudinal and shear sound velocities, density, elastic moduli, and Poisson's ratio were determined for polyurea at pressures to 13.5 GPa. By utilizing lower pressure dilatometry and lower frequency dynamic measurements, we corrected the high frequency Brillouin data for viscoelastic effects. Accordingly, the densities reported herein are more accurate than previous studies on other polymers; moreover, we show that the viscoelastic correction is generally applicable to Brillouin data. The glass transition at ambient temperature occurs at a relatively low $P_g \sim 1.1$ GPa. Because of the extreme strain-rate hardening of the polyurea when vitrification is imminent, the changes in properties upon solidification are more subtle in the high frequency Brillouin results than observed in conventional mechanical testing and dilatometry. The mechanical properties reported herein are of value in modeling polyurea under the high pressure, high loading rate conditions found in many applications of the material.

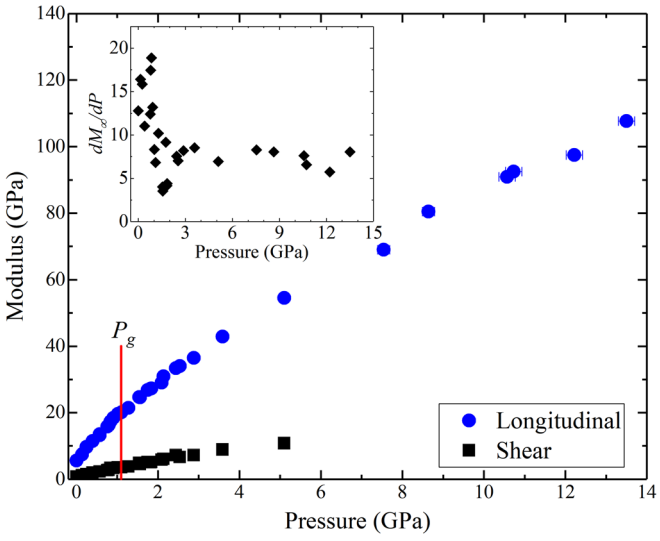

FIG. 6. High frequency longitudinal M_∞ and shear G_∞ moduli for polyurea. Vertical line denotes $P_g = 1.1$ GPa. Inset shows the pressure derivative of M_∞.

ACKNOWLEDGMENTS

The work at NRL was supported by the Office of Naval Research, in part by Code 332 (R.G.S. Barsoum). The Brillouin scattering measurements were performed at the Carnegie Institution of Washington, using facilities supported by the U.S. Department of Energy/National Security Administration (No. DE-NA-0002006, CDAC). T.C.R. acknowledges an American Society for Engineering Education postdoctoral fellowship. We thank D. Fragiadakis for a careful reading of the manuscript and insightful suggestions.

[1]C. M. Roland, S. Hensel-Bielowka, M. Paluch, and R. Casalini, Rep. Prog. Phys. **68**, 1405–1478 (2005).
[2]C. M. Roland, Macromolecules **43**, 7875 (2010).
[3]C. M. Roland, S. Bair, and R. Casalini, J. Chem. Phys. **125**, 124508 (2006).
[4]D. Coslovich and C. M. Roland, J. Phys. Chem. B **112**, 1329 (2008).
[5]C. M. Roland, J. L. Feldman, and R. Casalini, J. Non-Cryst. Sol. **352**, 4895 (2006).
[6]R. G. S. Barsoum, *Elastomeric Polymers with High Rate Sensitivity: Applications in Blast, Shockwave, and Penetration Mechanics* (William Andrew, 2015).
[7]N. Iqbal, M. Tripathi, S. Parthasarathy, D. Kumar, and P. Roy, RSC Adv. **6**, 109706 (2016).
[8]A. J. Hsieh, T. L. Chantawansri, W. Hu, K. E. Strawhecker, D. T. Casem, J. K. Eliason, K. A. Nelson, and E. M. Parsons, Polymer **55**, 1883–1892 (2014).
[9]T. Jiao, R. J. Clifton, and S. E. Grunschel, AIP Conf. Proc. **845**, 809–812 (2006).
[10]M. R. Amini, J. Isaacs, and S. Nemat-Nasser, Int. J. Impact Eng. **37**, 82–89 (2010).
[11]M. R. Amini and S. Nemat-Nasser, Int. J. Fract. **162**, 205–217 (2010).
[12]L. Xue, W. Mock, and T. Belytschko, Mech. Mater. **42**, 981–1003 (2010).
[13]V. Chakkarapani, K. Ravi-Chandar, and K. M. Liechti, J. Eng. Mater. Technol. **128**, 489–494 (2006).
[14]S. A. Tekalur, A. Shukla, and K. Shivakumar, Compos. Struct. **84**, 271–281 (2008).
[15]J. Yi, M. C. Boyce, G. F. Lee, and E. Balizer, Polymer **47**, 319–329 (2006).
[16]C. M. Roland, J. Twigg, Y. Vu, and P. H. Mott, Polymer **48**, 574–578 (2007).
[17]J. A. Pathak, J. N. Twigg, K. E. Nugent, D. L. Ho, E. K. Lin, P. H. Mott, C. G. Robertson, M. K. Vukmir, T. H. Epps, and C. M. Roland, Macromolecules **41**, 7543–7548 (2008).
[18]T. Choi, D. Fragiadakis, C. M. Roland, and J. Runt, Macromolecules **45**, 3581–3589 (2012).
[19]P. H. Mott, C. B. Giller, D. Fragiadakis, D. Rosenberg, and C. M. Roland, Polymer **105**, 227–233 (2016).
[20]P. W. Bridgman, Rev. Mod. Phys. **18**, 1 (1946).
[21]D. Walsh and P. Zoller, *Standard Pressure Volume Temperature Data for Polymers* (CRC Press, 1995).
[22]R. J. Hemley, High Pressure Res. **30**, 581–619 (2010).

[23]L. L. Stevens, E. B. Orler, D. M. Dattelbaum, M. Ahart, and R. J. Hemley, J. Chem. Phys. **127**, 104906 (2007).
[24]L. L. Stevens, D. M. Dattelbaum, M. Ahart, and R. J. Hemley, J. Appl. Phys. **112**, 023523 (2012).
[25]A. S. Benjamin, M. Ahart, S. A. Gramsch, L. L. Stevens, E. B. Orler, D. M. Dattelbaum, and R. J. Hemley, J. Chem. Phys. **137**, 014514 (2012).
[26]M.-S. Jeong, J.-H. Ko, Y. H. Ko, and K. J. Kim, Curr. Appl. Phys. **15**, 943–946 (2015).
[27]Y.-H. Ko, J. Min, and J. Song, Curr. Appl. Phys. **16**, 311–317 (2016).
[28]R. Meister, C. J. Marhoeffer, R. Sciamanda, L. Cotter, and T. Litovitz, J. Appl. Phys. **31**, 854–870 (1960).
[29]C. M. Roland, *Viscoelastic Behavior of Rubbery Materials* (Oxford, 2011).
[30]T. C. Ransom, M. Ahart, R. J. Hemley, and C. M. Roland, Macromolecules **50**, 8274–8278 (2017).
[31]I. L. Fabelinskii, *Molecular Scattering of Light* (Springer Science & Business Media, 2012).
[32]A. Polian, J. Raman Spectrosc. **34**, 633–637 (2003).
[33]G. J. Piermarini, S. Block, J. D. Barnett, and R. A. Forman, J. Appl. Phys. **46**, 2774–2780 (1975).
[34]B. W. Lee, M.-S. Jeong, J. S. Choi, J. Park, Y. H. Ko, K. J. Kim, and J.-H. Ko, Curr. Appl. Phys. **17**, 1396–1400 (2017).
[35]L. Comez, C. Masciovecchio, G. Monaco, and D. Fioretto, Solid State Phys. **63**, 1–77 (2012).
[36]R. B. Bogoslovov, C. M. Roland, and R. M. Gamache, Appl. Phys. Lett. **90**, 221910 (2007).
[37]C. M. Roland and R. Casalini, Polymer **48**, 5747–5752 (2007).
[38]L. Loubeyre, M. Ahart, S. A. Gramsch, and R. J. Hemley, J. Chem. Phys. **138**, 174507 (2013).
[39]P. H. Mott and C. M. Roland, Macromolecules **31**, 7095–7098 (1998).
[40]J. Qiao, A. V. Amirkhizi, K. Schaaf, S. Nemat-Nasser, and G. Wu, Mech. Mater. **43**, 598–607 (2011).
[41]W. F. Oliver, C. A. Herbst, S. M. Lindsay, and G. H. Wolf, Phys. Rev. Lett. **67**, 2795 (1991).
[42]M. Henkel, M. Pleimling, and R. Sanctuary, *Ageing and the Glass Transition* (Springer, 2007), Vol. 716.